

# Dynamics near a heteroclinic network

Manuela A.D. Aguiar †‡ Sofia B.S.D. Castro †‡ Isabel S. Labouriau †  
*maguiar@fep.up.pt*      *sdcastro@fep.up.pt*      *islabour@fc.up.pt*

† Centro de Matemática da Universidade do Porto; Rua do Campo Alegre, 687; 4169-007 Porto; Portugal

‡ Faculdade de Economia, Universidade do Porto; Rua Dr. Roberto Frias; 4200-464 Porto; Portugal

ABSTRACT. We study the dynamical behaviour of a smooth vector field on a 3-manifold near a heteroclinic network. Under some generic assumptions on the network, we prove that every path on the network is followed by a neighbouring trajectory of the vector field – there is switching on the network. We also show that near the network there is an infinite number of hyperbolic suspended horseshoes. This leads to the existence of a horseshoe of suspended horseshoes with the shape of the network.

Our results are motivated by an example constructed by Field (*Lectures on Bifurcations, Dynamics, and Symmetry*, Pitman Research Notes in Mathematics Series 356, Longman, 1996) where we have observed, numerically, the existence of such a network.

AMS classification scheme numbers: 37C10, 37C29, 37C80, 37D45, 37C50, 34F05

## 1. INTRODUCTION

Heteroclinic phenomena, such as cycles and networks, have attracted the attention of many authors in the last 25 years. It has been observed that these phenomena are often associated with complex dynamics. Although there are many results on the dynamics arising from the existence of heteroclinic cycles there are still very few analytic results concerning dynamic behaviour induced by a network in its vicinity. These are the main concern of this paper.

We shall think of a *heteroclinic cycle* as a cycle of (relative) equilibria connected by non-trivial intersections of their invariant manifolds. In this case we say there is a *connection* between the equilibria. Nearby trajectories may follow along the connections.

In some examples there is more than one heteroclinic cycle for the same dynamical system. When coexisting heteroclinic cycles have a nonempty intersection we talk about a *heteroclinic network*.

If there are trajectories following along all the sequences of connections in the network, we say there is *switching* on the network.

We prove switching under generic assumptions on a network. Our approach also shows the existence of a horseshoe of suspended horseshoes with the shape of the network.

There have been examples of robust heteroclinic cycles involving periodic trajectories as well as equilibria, using various symmetry groups and settings. Symmetry is a natural setting for the existence of persistent heteroclinic cycles since, as shown by Field [11] in 1980, symmetry can force non-transversal intersections of invariant manifolds. If the connections between the (relative) equilibria in the cycle are contained in fixed-point spaces, the invariance of these spaces guarantees robustness of the cycle. A review of results on robust heteroclinic cycles up to 1997 can be found in Krupa [21]. See Chossat *et al* [9], Ashwin and Chossat [4], Field and Swift [14] and Dias *et al* [10] for more recent developments.

The phenomenon of bifurcation from heteroclinic cycles is studied by Campbell and Holmes [7] and Worfolk [28]. In the work of Worfolk, complicated dynamics in the neighbourhood of a perturbed heteroclinic cycle appears due to the existence of Smale horseshoes embedded in the flow. A review of results on the dynamical consequences of some homoclinic and heteroclinic motions in three and four dimensions is described by Wiggins [27].

Early examples of heteroclinic networks may be found in Melbourne *et al* [23], Silber *et al* [26], Lauterbach and Roberts [22], Field and Richardson [13], Ashwin and Field [5] and Kirk and Silber [20].

The last authors raise two questions. The first concerns the stability of the heteroclinic cycles that form the network. This issue is also

addressed by Brannath [6] who provides necessary and sufficient conditions for heteroclinic cycles to be *relatively* asymptotically stable – given that being part of a network prevents them from being asymptotically stable attractors. The second question concerns the dynamics associated with the existence of the heteroclinic network. They conjecture the existence of random switching between the cycles of the network in case the “dynamics along the network include sequences of visits to the equilibria more complicated than those associated with a simple heteroclinic cycle”. We prove this conjecture for certain heteroclinic networks.

An example of switching appears in Guckenheimer and Worfolk [18]. In 2003, the phenomenon of switching was introduced by Armsbruster *et al* [3] as noise-induced. We show the existence of switching without noise.

Numerical evidence of complex behaviour near a network was observed by, for example, Field [15] and Chawanya [8]. An analytic approach appears in Reissner [24] using the context of time-reversible systems, partly to simplify the analysis. We address the problem analytically without the use of reversing-symmetries.

In Appendix A of [15], Field conjectures that a given dynamical system in  $\mathbf{R}^4$  possesses a network of heteroclinic cycles leading to horseshoe dynamics. These conjectures and further discussions with Field, motivated our study of the dynamical system that we present here. We prove Field’s conjectures concerning the dynamics and the existence of switching for this example, assuming the existence of numerically observed connections. Our results hold under general assumptions and are therefore not strictly about Field’s example.

We conclude this introduction with a description of our results and of their presentation.

**Framework of the paper.** In the next section we present and discuss some definitions which will be used throughout this paper. The following section contains the description of the dynamical system in Appendix A of Field [15] and its symmetries. Numerical evidence of the connections and the way symmetry can be used to generate the network are described in sections 4 and 5, respectively. The connections between saddles are obtained by numerical integration of the dynamical system. We then use the symmetry of the system to show how all observed connections can be obtained using the group action on a selected set of numerically observed connections. In section 5, we also use symmetry to reduce the original network to a quotient network which will be used in subsequent sections.

Section 6 starts with a technical description of the geometry of the Poincaré map near the connections. This is then used to establish switching and dynamics-related results. Assuming the existence of the

heteroclinic connections, we prove: the existence of horseshoe dynamics in a neighbourhood of heteroclinic cycles in the network; switching both at every node of the network; and switching on the network. Beyond the initial conjectures of Field, the existence of switching on the network amounts to proving that all the connections of the network are realized by nearby dynamics. These proofs rely on some general hypotheses on the dynamical system (which are satisfied by generic systems besides the one studied in [15]). We make a couple of more restrictive hypotheses to include some resonances present in this particular dynamical system. The resonance-related hypotheses are not essential for the proof, which holds without them although with dirtier calculations. We also note that although for Field's example there are two pairs of complex eigenvalues, one pair is enough to guarantee the existence of switching and horseshoes.

The results of section 6 are presented in five subsections. In the first subsection we show the existence of switching at every node of the quotient network. In the following two subsections, we prove the existence of suspended horseshoe dynamics in the neighbourhood of heteroclinic cycles of the quotient network, with all the usual consequences for the dynamics. In actual fact, we prove that there exists an infinite number of hyperbolic suspended horseshoes. Subsection 6.3 contains the proof of the hyperbolicity of the Poincaré map. This guarantees that invariant sets persist under symmetry-breaking perturbations. Hence, the horseshoes and switching persist generically. Switching on the network is proved in subsection 6.4 and we relate the results obtained to the notion of shadowing in the last subsection of section 6.

The final section of this paper is devoted to showing how results obtained for the quotient network translate to the original setting. We show that the switching obtained in the quotient network can be lifted to the original network, thus proving that all the connections of the original network are realized by the dynamics.

## 2. PRELIMINARIES

Let  $X$  be a smooth vector field on  $\mathbf{R}^m$ .

Suppose that  $A$  is a compact invariant set for the flow of  $X$ . Following [15] we say that  $A$  is an *invariant saddle* if both  $\overline{W^s(A)} \setminus A$  and  $\overline{W^u(A)} \setminus A$  contain  $A$ . Notice that invariant saddles do not have to be hyperbolic, although in our example they are.

We say saddles  $A_1$  and  $A_2$  are a *pair of connected saddles* if there exists a connection from  $A_1$  to  $A_2$ . A *connection* from saddle  $A_1$  to saddle  $A_2$  (denoted  $[A_1 \rightarrow A_2]$ ) is any one of the trajectories contained in  $W^u(A_1) \cap W^s(A_2)$ .

Let  $\{A_i, i = 0, \dots, n-1\}$  be a finite ordered set of mutually disjoint invariant saddles for the vector field  $X$ . If there are connections  $[A_i \rightarrow$

$A_{i+1}]$  for  $i = 0, \dots, n-1 \pmod{n}$  then we say that

$$\cup_{i=0}^{n-1} A_i \cup [A_i \rightarrow A_{i+1}]$$

is the *heteroclinic cycle* determined by  $\{A_i\}$ .

We think of a *heteroclinic network*, usually denoted by  $\Sigma$ , as a finite union of heteroclinic cycles. The saddles defining the heteroclinic cycles and network are called *nodes* of the network and we denote them by  $n_i$ . We define a *subnetwork* as a network consisting of the union of fewer cycles, not necessarily involving a smaller number of nodes. We shall assume that the network is connected. The disconnected case is a disjoint union of connected networks.

This is a loose definition. In the literature, several definitions have appeared, mostly due to the different needs of the issues addressed. See Field and Richardson [13], Field [15], Kirk & Silber [20] and Dias *et al* [10] where the expressions *web*, *complex* and *network* are used for roughly the same concept.

Ashwin & Field present in [5] a definition of heteroclinic network that generalizes the definitions of heteroclinic network thus far, and introduce the concept of depth in the network. They define a heteroclinic network as a flow-invariant set that is indecomposable but not recurrent.

Their definition covers many previously discussed examples of heteroclinic behaviour but not the Shilnikov network of Field's example in ([15], appendix A) that we study here as we establish the existence of an infinite set of recurrent points in the neighbourhood of the network.

Let  $\Sigma$  be a network with a finite set of nodes. We define a *path* on  $\Sigma$  as a bi-infinite sequence  $(c_j)_{j \in \mathbf{Z}}$  of connections in  $\Sigma$  such that  $c_j = [n_{j-1} \rightarrow n_j]$ , with  $n_j$  nodes of  $\Sigma$ .

We say there is *switching at a node*  $n$  if, for any neighbourhood of a point in a connection leading to node  $n$ , trajectories starting in that neighbourhood will follow along all the possible connections forward from  $n$ .

Let  $N_\Sigma$  be any neighbourhood of a network  $\Sigma$  and  $U_n$  arbitrary neighbourhoods of the nodes  $n \in \Sigma$ . For every connection contained in  $\Sigma$ , let  $p$  be an arbitrary point on it and consider an arbitrary neighbourhood  $U_p$  of each  $p$ . We say there is *switching on the network* if, for each path  $(c_i)_{i \in \mathbf{Z}}$  contained in  $\Sigma$ , there is a trajectory  $x(t) \subset N_\Sigma$  and sequences  $(t_i), (s_i)$  with  $t_{i-1} < s_i < t_i$  such that  $x(s_i) \in U_{p_i}$  and  $x(t_i) \in U_{n_i}$ , where  $p_i \in c_i$ .

We remark that switching at every node is not enough to guarantee the existence of switching on the network. In fact, the latter is a much stronger concept.

### 3. EQUATIONS AND SYMMETRIES

Consider the family of differential equations in  $\mathbf{R}^4$ , given by:

$$(1) \quad \begin{cases} \dot{x}_1 &= \lambda x_1 - |x|^2 x_1 + \beta(x_1^2 x_2 - y_1^2 x_2 - 2x_1 y_1 y_2) + \gamma(x_2^3 - 3x_2 y_2^2) \\ \dot{y}_1 &= \lambda y_1 - |x|^2 y_1 + \beta(-x_1^2 y_2 + y_1^2 y_2 - 2x_1 y_1 x_2) + \gamma(-y_2^3 + 3x_2^2 y_2) \\ \dot{x}_2 &= \lambda x_2 - |x|^2 x_2 + \beta(x_1 x_2^2 - x_1 y_2^2 + 2y_1 x_2 y_2) + \gamma(x_1^3 - 3x_1 y_1^2) \\ \dot{y}_2 &= \lambda y_2 - |x|^2 y_2 + \beta(y_1 x_2^2 - y_1 y_2^2 - 2x_1 x_2 y_2) + \gamma(y_1^3 - 3x_1^2 y_1) \end{cases}$$

with  $x = (x_1, y_1, x_2, y_2)$  and real parameters  $\lambda$ ,  $\beta$  and  $\gamma$ . These equations are studied by Field [15] as a counterexample to the maximal isotropy subgroup conjecture. We describe some of its properties and refer the reader to appendix A of [15] for more details.

Identifying  $\mathbf{R}^4 \approx \mathbf{C}^2$  we may rewrite the equations in complex coordinates  $(z_1, z_2)$  where  $z_j = x_j + iy_j, j = 1, 2$ . With this notation, the family (1) is equivariant by the discrete group  $\Gamma$  of order 40 generated by

$$(2) \quad \begin{aligned} s(z_1, z_2) &= (\omega z_1, \omega^2 z_2), & \text{of order 5,} \\ t(z_1, z_2) &= (\bar{z}_2, z_1), & \text{of order 4,} \\ -I(z_1, z_2) &= (-z_1, -z_2), \end{aligned}$$

where  $\omega = e^{\frac{2\pi i}{5}}$ . We denote by  $\langle g \rangle$  the subgroup generated by an element  $g \in \Gamma$ . There are five copies of each of the following proper fixed-point spaces ([15], Lemma A.7):

$$\begin{aligned} L_1 &= \text{Fix}(\langle t \rangle) = \{(x_1, 0, x_1, 0) : x_1 \in \mathbf{R}\} \\ L_2 &= \text{Fix}(\langle -t \rangle) = \{(x_1, 0, -x_1, 0) : x_1 \in \mathbf{R}\} \\ P_1 &= \text{Fix}(\langle t^2 \rangle) = \{(x_1, 0, x_2, 0) : x_1, x_2 \in \mathbf{R}\} \\ P_2 &= \text{Fix}(\langle -t^2 \rangle) = \{(0, y_1, 0, y_2) : y_1, y_2 \in \mathbf{R}\}. \end{aligned}$$

From now on we fix parameter values as follows:

$$(3) \quad \lambda > 0, \quad \gamma < 0, \quad \beta > 0, \quad \gamma + 3\beta > 0 \quad \text{and} \quad |\beta + \gamma| < 2.$$

For these parameter values the cubic term of (1) is contracting (Lemma A.10 of [15]). By the Invariant Sphere Theorem ([12], [15]) the dynamics of (1) can be reduced to an invariant three-dimensional sphere that is globally attracting in the sense that every trajectory except the trivial equilibrium is forward asymptotic to the sphere. The invariant sphere can be obtained as the graph of a function from the unit sphere in  $\mathbf{R}^4$  into  $\mathbf{R}^+$ . In the particular case  $\beta = -\gamma$  this function is constant and thus the topological sphere is indeed the geometric sphere of radius  $\sqrt{\lambda}$ . We restrict our attention to the flow on the topological sphere, denoted  $S^3$ .

The following results on the dynamics on the fixed-point spaces are relevant for later sections.

- Each one of the axes  $L_1$  and  $L_2$  meets  $S^3$  at two equilibria,  $\pm a(\lambda)$  and  $\pm b(\lambda)$  respectively. These are the only nontrivial equilibria on  $P_1$  ([15], Lemma A.11).

- For the flow restricted to  $P_1$ , the points  $\pm b(\lambda)$  are sinks,  $\pm a(\lambda)$  are saddles ([15], Lemma A.14); see figure 1.a).
- The intersection of  $S^3$  with the plane  $P_1$  consists of four arcs formed by trajectories joining  $\pm a(\lambda)$  to  $\pm b(\lambda)$ ; see figure 1.a).
- In the restriction to  $S^3$ ,  $\dim(W^u(b(\lambda))) = 2$  and  $\dim(W^s(a(\lambda))) = 2$  and both  $W^u(b(\lambda))$  and  $W^s(a(\lambda))$  are transverse to the plane  $P_1$  ([15], Lemma A.14).
- There are no nontrivial equilibria on the plane  $P_2$  ([15], Proposition A.15). The intersection of  $P_2$  and  $S^3$  is a periodic trajectory,  $c(\lambda)$ , that attracts all points in  $P_2 - \{0\}$ .
- The only equilibria of (1) are the origin,  $\pm s^n a(\lambda)$  and  $\pm s^n b(\lambda)$  ( $n = 0, \dots, 4$ ).

The dynamics in the conjugates by  $\Gamma$  of these fixed-point spaces is similar.

Field conjectures the existence of a heteroclinic network involving  $a(\lambda)$ ,  $b(\lambda)$ ,  $c(\lambda)$  and all their conjugates and that there is chaotic dynamics near the network. Numerical evidence for such a network is discussed in the following two sections. The existence of chaotic dynamics near the network is left for the last sections.

#### 4. NUMERICAL EVIDENCE OF CONNECTIONS

From now on we assume  $\lambda = 1$  fixed and we omit references to  $\lambda$  in the text, using  $a = a(1)$ ,  $b = b(1)$ ,  $c = c(1)$ .

In our numerical study we used the dynamical systems package Dstool(Dynamical systems toolkit) [17], incorporating a C-routine of Aguiar [1]. For each Dstool computation of a trajectory, with given initial conditions, the C-routine gives as output a sequence that identifies the invariant saddles near the trajectory. See [1] for details, including the C-routine.

The sequences produced give evidence of the existence of several connections. We single out the following:

- $[a \rightarrow b]$  (also found analytically)
- $[b \rightarrow \pm s(a)]$
- $[b \rightarrow c]$
- $[b \rightarrow sc]$
- $[c \rightarrow a]$
- $[c \rightarrow sa]$
- $[c \rightarrow sc]$

with  $s$  the element of  $\Gamma$  defined in (2).

As we show in the next section, the connections listed above, together with the symmetry of the problem, suffice to produce all the connections observed numerically as well as to construct a heteroclinic network  $\Sigma$ .

Note that we do not know the multiplicity of these connections. This seems to be impossible to determine numerically.

The periodic trajectory  $c$  on the plane  $P_2$  is a hyperbolic saddle whose unstable manifold may have dimension 2 or 3. Numerical computations with GAIO(Global Analysis of Invariant Objects) (Junge [19]) indicate that the unstable manifold of the periodic trajectory is two-dimensional.

In the cases where invariant manifolds of dimension  $\geq 2$  of two equilibria intersect, numerical computations with GAIO indicate that the intersection is transversal.

## 5. SYMMETRIES AND HETEROCLINIC NETWORKS

Given a connection in (1), the symmetry can be used to obtain other connections. When applied to the connections obtained numerically, it produces a heteroclinic network.

Let  $X$  be a smooth vector field on  $\mathbf{R}^m$ . Consider a pair of connected saddles  $A_1, A_2$  for  $X$ . Let  $\Gamma$  be a discrete Lie group acting on  $\mathbf{R}^m$ . If  $X$  is  $\Gamma$ -equivariant, then for  $g \in \Gamma$  we have

$$W^u(g.A_1) \cap W^s(g.A_2) = g.(W^u(A_1) \cap W^s(A_2)).$$

Thus we have an action of  $\Gamma$  in the set consisting of pairs of connected saddles together with the connections between them. The group  $\Gamma$  acts on  $\Gamma(A_1) \times \Gamma(A_2)$  by  $g.(A_1, A_2) = (g.A_1, g.A_2)$ . The connections we can obtain by symmetry from  $[A_1 \rightarrow A_2]$  may be identified with  $(A_i, A_j)$  in the group orbit  $\Gamma((A_1, A_2))$ . Let  $\Gamma_{A_i}$  be the isotropy subgroup of  $A_i$ . Since  $(A_1, A_2)$  has isotropy subgroup  $\Gamma_{A_1} \cap \Gamma_{A_2}$ , the order of the group orbit  $\Gamma((A_1, A_2))$  is

$$(4) \quad \#\Gamma / \#(\Gamma_{A_1} \cap \Gamma_{A_2}).$$

For the group  $\Gamma$  and the saddles  $a, b, c$  of section 3 the isotropy subgroups and orbits are listed in table 1.

saddle	group orbit	isotropy subgroup
$a$	$\{\pm s^n a\}$	$\langle t \rangle$
$b$	$\{\pm s^n b\}$	$\langle -t \rangle$
$c$	$\{s^n c\}$	$\langle -I, t \rangle$

TABLE 1. Isotropy subgroups and orbits for the saddles  $a, b, c$  of (1).

The 220 pairs of connected saddles listed in table 2 were obtained by computing the  $\Gamma$  orbits of the pairs of section 4. No other pairs of connected saddles were found numerically.

As an illustration on the use of symmetry to obtain new connections, we derive the second row of table 2. The isotropy subgroups for  $b$  and  $sa$  can be read from table 1 and using the relation  $ts^2 = st$  so that we get  $\Gamma_{sa} = \langle ts \rangle$ . Thus,  $\Gamma_b \cap \Gamma_{sa} = \langle -t \rangle \cap \langle ts \rangle = \{I\}$ . Starting with  $[b \rightarrow sa]$ , there are 40 pairs of connected saddles that may be obtained by symmetry, by (4). In particular,  $[b \rightarrow sa]$  is mapped by  $-t$  into  $[b \rightarrow -s^3a]$  (using  $s^3t = ts$ ), by  $t^2$  into  $[b \rightarrow s^4a]$  and by  $-t^3$  into  $[b \rightarrow -s^2a]$ . Applying  $\pm s^k$  to these pairs of connected saddles and repeating the procedure with  $[b \rightarrow -sa]$  we obtain the second row of table 2.

original connection	new connections	conditions	total number of different connections
$[a \rightarrow b]$	$\pm s^n[a \rightarrow \pm b]$	$n \in \mathbf{Z}_5$	20
$[b \rightarrow \pm sa]$	$\pm s^k[b \rightarrow \pm s^n a]$	$k, n \in \mathbf{Z}_5, n \neq 0$	80
$[b \rightarrow c]$	$s^n[\pm b \rightarrow c]$	$n \in \mathbf{Z}_5$	10
$[b \rightarrow sc]$	$s^k[\pm b \rightarrow s^n c]$	$k, n \in \mathbf{Z}_5, n \neq 0$	40
$[c \rightarrow a]$	$s^n[c \rightarrow \pm a]$	$n \in \mathbf{Z}_5$	10
$[c \rightarrow sa]$	$s^k[c \rightarrow \pm s^n a]$	$k, n \in \mathbf{Z}_5, n \neq 0$	40
$[c \rightarrow sc]$	$s^k[c \rightarrow s^n c]$	$k, n \in \mathbf{Z}_5, n \neq 0$	20

TABLE 2. New connections between pairs of connected saddles generated by symmetry.

**Theorem 1.** *Consider a vector field  $X$  having invariant saddles  $a$ ,  $b$ , and  $c$  and the original connections in the first column of table 2. Let  $\Gamma$  be the finite group of section 3. If  $X$  is  $\Gamma$ -equivariant, then it has a heteroclinic network  $\Sigma$  involving all the invariant saddles of  $\Gamma(\{a, b, c\})$  and all the pairs of connected saddles in table 2.*

**Proof:** Since the symmetry group is finite, given the original connections we get by symmetry a finite number of connections which are given in table 2. For each invariant saddle there is at least one connection starting and at least one connection ending at that saddle. Thus there are sequences of connections starting and ending at the same invariant saddle and every connection belongs to at least one of those sequences. Each sequence of connections gives a heteroclinic cycle. The union of all the heteroclinic cycles is a heteroclinic network involving all the invariant saddles of equations (1).  $\square$

If there are more connections involving the saddles of  $\Gamma(\{a, b, c\})$  then, by the same method, we obtain a larger network of which  $\Sigma$  (in theorem 1) is a subnetwork.

**Remark:** The pairs of connected saddles in  $\Gamma(\{a, b, c\}) \times \Gamma(\{a, b, c\})$  that were *not* found correspond to:

- all the connections  $[g_1 a \rightarrow g_2 x]$  with  $x = a, c$ ;
- all the connections  $[g_1 x \rightarrow g_2 b]$  with  $x = b, c$ ;
- $\Gamma[a \rightarrow \pm sb]$  i.e.  $\pm s^k[a \rightarrow \pm s^n b]$ ;
- $\Gamma([b \rightarrow a])$  i.e.  $\pm s^k[b \rightarrow \pm a]$ ;
- $\Gamma([c \rightarrow c])$  i.e.  $s^k[c \rightarrow c]$  ;

where  $g_1, g_2$  are arbitrary elements of  $\Gamma$ ,  $k, n \in \mathbf{Z} \pmod{5}$  and  $n \neq 0$ .

**5.1. Quotient network.** Suppose there are no connections besides those of table 2 and that there is only one connection for each pair of connected saddles. A considerable simplification is obtained if we restrict our attention to the subnetwork corresponding to the conjugates of the equilibria  $a, b$ . This reduces the number of pairs of connected saddles from 220 to 100. The subnetwork of equilibria is already interesting from the point of view of the dynamics and, henceforth, we restrict our attention to this subnetwork.

A further reduction consists in identifying some of the points in a group orbit, as we proceed to describe.

The subgroup  $G = \langle s, -I \rangle \subset \Gamma$  acts freely on  $\mathbf{R}^4$  and on the invariant sphere  $S^3$ . We work on the orbit space  $S^3/G$ , a three-dimensional manifold. The restriction of (1) to  $S^3$  defines a quotient vector field on  $S^3/G$ . The subgroup  $H = \langle -t \rangle \subset \Gamma$  induces a (non-free) action on  $S^3/G$ .

The invariant circles with four equilibria in the group orbit of  $S^3 \cap \text{Fix}(\langle t^2 \rangle)$  by  $\Gamma$  drop down to an  $H$ -invariant circle with two equilibria  $A, B$  in  $S^3/G$  (see figure 1). Note that these equilibria correspond, respectively, to the group orbits  $\Gamma(a)$  and  $\Gamma(b)$ , since  $ta = a$  and  $tb = -b$ . The equilibria  $A$  and  $B$  are fixed by  $H$  and semicircles are interchanged by  $H$ . More importantly, the group  $H$  acts freely on the two-dimensional stable and unstable manifolds of  $A$  and  $B$ .

Thus, the 20 connections in  $S^3$  forming the  $G$ -orbit of the two connections  $[a \rightarrow \pm b]$  drop down to two connections from  $A$  to  $B$  in  $S^3/G$ .

Consider one of the connection  $[b \rightarrow sa]$ . As we have already seen its  $H$ -orbit has four elements. The  $G$ -orbit of these four connections consists of 40 connections in  $S^3$  that drop down to four connections from  $B$  to  $A$  in  $S^3/G$  (given by the action of  $H$ ). Yet another four connections drop down from the 40 pairs in the orbit of  $[b \rightarrow -sa]$ .

In conclusion, the heteroclinic network between the 20 equilibria in  $S^3$  drops down, by the reduction to the orbit space  $S^3/G$ , to a quotient heteroclinic network between the two equilibria  $A$  and  $B$ . There are two connections from  $A$  to  $B$  and eight connections from  $B$  to  $A$  as shown in figure 1. These are representatives of all the connections in the subnetwork of equilibria.

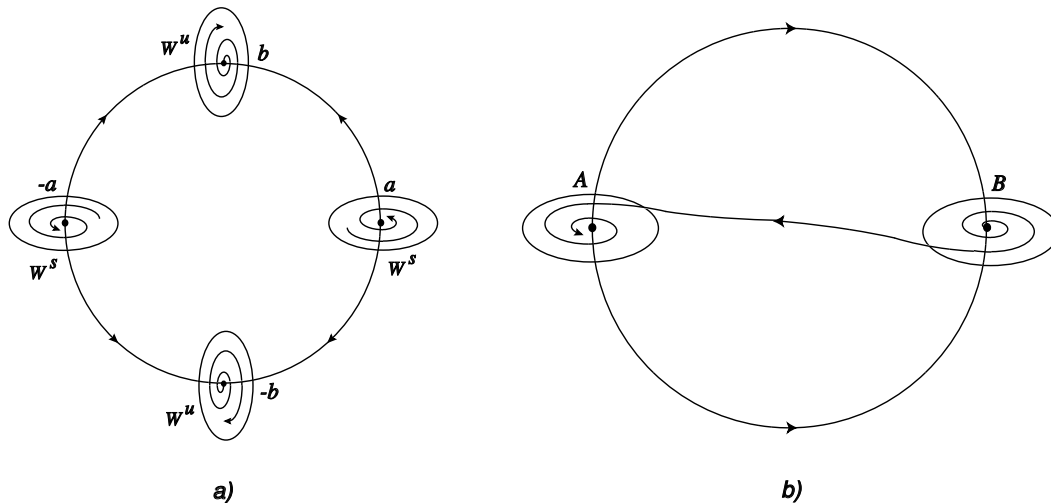


FIGURE 1. a) Dynamics of Field's example near the plane  $P_1$  (similar to figure 11 in [15]). b) Schematic representation of the quotient subnetwork of equilibria. The line from  $B$  to  $A$  represents 8 connections.

## 6. THE POINCARÉ MAP

In this section we describe the geometry of the flow in a neighbourhood of a network involving two equilibria  $A$ ,  $B$ , like the quotient network of subsection 5.1. We are concerned with persistent behaviour and thus many of the calculations are illustrated for a particular case. The results hold for any network with a similar structure, so we state the properties that are going to be used.

(H0) Let  $X$  be a smooth vector field in a 3-manifold with two equilibria  $A$ ,  $B$ .

Let  $\lambda_e$  and  $\alpha_e \pm i\beta_e$  be the eigenvalues of the linearization of  $X$  at  $e = A, B$ . We consider

$$(H1) \quad \lambda_A > 0, \quad \alpha_A < 0, \quad \beta_A > 0, \quad \lambda_B < 0, \quad \alpha_B > 0, \quad \beta_B > 0,$$

$$(H2) \quad -\alpha_A \beta_B = \beta_A \alpha_B,$$

$$(H3) \quad \frac{\alpha_A \lambda_B}{\lambda_A \alpha_B} = 1.$$

Hypotheses (H1) (H2) and (H3) are satisfied at the equilibria of (1). The results of this paper still hold if the eigenvalues do not satisfy (H2) and (H3), with slightly more complicated proofs.

A saddle with a pair of complex eigenvalues in  $\mathbf{R}^3$  will not have resonances of order 1. By theorem 1 in Samovol [25], the flow is  $C^1$  linearizable around each equilibrium. In fact, the only obstruction to

$C^1$  linearization would come from terms of degree 2, which do not exist here.

In neighbourhoods  $N_e$  of  $e$ ,  $e = A, B$  we choose coordinates for which the flow is linear, with the equilibrium at the origin and such that the local stable and unstable manifolds are either the horizontal plane or the vertical axis. Using polar coordinates  $r, \theta$  in the horizontal plane and  $z$  for the vertical axis, we have for  $A$ :

$$\begin{aligned} W_{loc}^u(A) &= \{(0, 0, z) \mid z \in \mathbf{R}\} \\ W_{loc}^s(A) &= \{(r, \theta, 0) \mid r \in \mathbf{R}^+, \theta \in [-\pi, \pi]\} \end{aligned}$$

and for  $B$ :

$$\begin{aligned} W_{loc}^s(B) &= \{(0, 0, z) \mid z \in \mathbf{R}\} \\ W_{loc}^u(B) &= \{(r, \theta, 0) \mid r \in \mathbf{R}^+, \theta \in [-\pi, \pi]\}. \end{aligned}$$

Inside each neighbourhood  $N_e$ ,  $e = A, B$  we consider cylindrical neighbourhoods of the equilibria, delimited by the surfaces:

$$\begin{aligned} \mathcal{W}_e &= \{(r, \theta, z) \mid r = r_e, \theta \in [-\pi, \pi] \text{ and } -z_e < z < z_e\}, \\ \mathcal{T}_e &= \{(r, \theta, z) \mid r < r_e, \theta \in [-\pi, \pi] \text{ and } z = z_e\}, \\ \mathcal{B}_e &= \{(r, \theta, z) \mid r < r_e, \theta \in [-\pi, \pi] \text{ and } z = -z_e\}. \end{aligned}$$

With this notation the network of section 5.1 corresponds to the assumptions:

- (H4) The flow connects the positive half-axis  $z^+ = \{(0, 0, z) \mid z > 0\}$  in  $N_A$  to the positive half-axis  $z^+$  in  $N_B$  and the negative half-axis  $z^-$  in  $N_A$  to the negative half-axis  $z^-$  in  $N_B$ . These are the only connections  $[A \rightarrow B]$ .
- (H5) The flow from  $\mathcal{T}_A$  and  $\mathcal{B}_A$  follows these connections in flow-box fashion. Roughly speaking, it maps  $\mathcal{T}_A$  into  $\mathcal{T}_B$  and  $\mathcal{B}_A$  into  $\mathcal{B}_B$ .
- (H6) There are exactly  $m$  connections from  $W_{loc}^u(B)$  to  $W_{loc}^s(A)$  and the two-dimensional manifolds meet transversely at these connections. The flow from  $\mathcal{W}_B$  to  $\mathcal{W}_A$  follows these connections in flow-box fashion in suitable neighbourhoods of the connections.

In  $N_A$  and  $N_B$ , let  $\mathcal{W}_{e_0}$ ,  $e = A, B$  be given by

$$\mathcal{W}_{e_0} = \{(r, \theta, z) \mid r = r_e \text{ and } z = 0\},$$

i.e.,  $\mathcal{W}_{A_0} = W_{loc}^s(A) \cap \mathcal{W}_A$  and  $\mathcal{W}_{B_0} = W_{loc}^u(B) \cap \mathcal{W}_B$ . Assumption (H6) means that exactly  $m$  points in the circle  $\mathcal{W}_{B_0}$  are mapped by the flow into  $m$  points in  $\mathcal{W}_{A_0}$ .

Let  $p_1, p_2 \in \mathcal{W}_{A_0}$  be two of these connection points (possibly the same) and consider neighbourhoods  $p_1 \in R_1$  and  $p_2 \in R_2$  in  $\mathcal{W}_A$ . Suppose  $R_1 \cap R_2 = \emptyset$  if  $p_1 \neq p_2$  and  $R_1 = R_2$  if  $p_1 = p_2$ .

In what follows we define a Poincaré map  $\Psi$  for the points in  $R_1$  whose image by the flow follows the connection of the positive half-axes in (H4) and then returns to  $R_2$  along one of the connections in (H6). The Poincaré map will be the composition of transition maps

(see Figure 2)  $\Psi = \phi_{BA} \circ \varphi_B \circ \phi_{AB} \circ \varphi_A$ , that are locally defined in neighbourhoods of the connections. The maps are not defined at all points of the walls  $\mathcal{W}_e$  and tops  $\mathcal{T}_e$  of the cylinders, nor for the whole neighbourhood  $R_1$ , but roughly speaking they are as in Figure 2:

$$\varphi_A : \mathcal{W}_A^+ \rightarrow \mathcal{T}_A \quad \varphi_B : \mathcal{T}_B \rightarrow \mathcal{W}_B^+$$

where

$$\mathcal{W}_e^+ = \{(r, \theta, z) \mid r = r_e \text{ and } z > 0\}; \quad e = A, B$$

and

$$\phi_{AB} : \mathcal{T}_A \rightarrow \mathcal{T}_B \quad \phi_{BA} : \mathcal{W}_B \rightarrow \mathcal{W}_A.$$

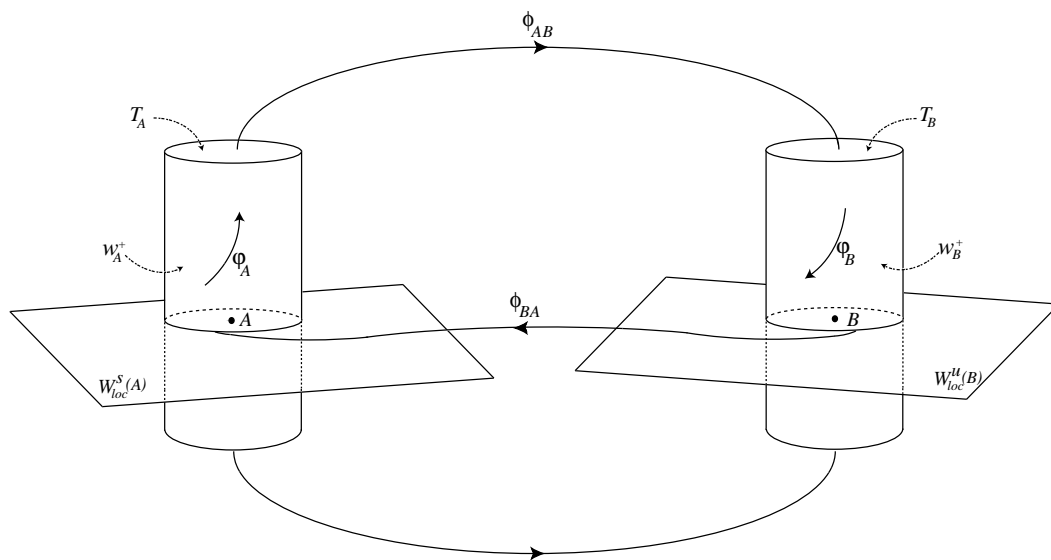


FIGURE 2. Transition maps  $\varphi_B$ ,  $\phi_{AB}$ ,  $\varphi_A$ ,  $\phi_{BA}$ .

A similar return map can be defined when the flow goes through the bottom  $\mathcal{B}_e$  of the cylinders with analogous results. First we explore the transition  $\Phi = \varphi_B \circ \phi_{AB} \circ \varphi_A$ , from  $\mathcal{W}_A^+$  to  $\mathcal{W}_B^+$ .

For  $e = A, B$  we parametrize the cylinder walls  $\mathcal{W}_e$ ,  $e = A, B$  by  $(x, y) \mapsto (r_e, x, y) = (r_e, \theta, z)$  with  $x \in \mathcal{W}_{e_0}$  being the azimuthal direction  $\theta$ . The cylinder tops  $\mathcal{T}_e$  are parametrized in polar coordinates by  $(r, \theta) \mapsto (r, \theta, z_e)$ ,  $r > 0$ . For  $p = (x_0, 0) \in \mathcal{W}_{e_0}$  we define a *rectangle centered at p* as the set

$$R_p = \{(x, u) : -w \leq x - x_0 \leq w \quad \text{and} \quad -y_0 \leq u \leq y_0\} \subset \mathcal{W}_e$$

with height  $y_0$ ,  $0 < y_0 < z_e$ , and width  $w$ ,  $0 < w \ll \pi$ . Their interiors form a basis for an open cover of  $\mathcal{W}_{e_0}$ . The *positive rectangle centered at p* will be  $R_p^+ = R_p \cap \mathcal{W}_e^+$ .

**Proposition 2.** *Let  $X$  be a vector field satisfying (H0–H6). Let  $p \in \mathcal{W}_{A_0}$  and  $q \in \mathcal{W}_{B_0}$  be two points in the connections  $[B \rightarrow A]$  (not necessarily in the same connection) and let  $\Phi = \varphi_B \circ \phi_{AB} \circ \varphi_A$ . Given rectangles  $R_p \subset \mathcal{W}_A$  centered at  $p$  and  $R_q \subset \mathcal{W}_B$  centered at  $q$  then  $\Phi(R_p^+) \cap R_q \neq \emptyset$ . Moreover, in suitable coordinates in  $R_p$  and  $R_q$ , there are constants  $c_1, c_2$ , with  $c_1 < 0$ , such that:*

$$\Phi(x, y) = (\Phi_1(x, y), \Phi_2(x, y)) = (x + c_1 \ln y + c_2, y).$$

**Proof:** Choose coordinates  $(x, y)$  in  $\mathcal{W}_A$  as above, with  $p$  at the origin  $x = y = 0$ . It is sufficient to show the result for  $R_p$  and  $R_q$  arbitrary rectangles centered at  $p$  and  $q$  respectively.

Since the flow has been linearized in  $N_e$  and using (H1) the expressions for  $\varphi_e$  in these coordinates are:

$$(5) \quad \varphi_A(x, y) = \left( r_A \left( \frac{y}{z_A} \right)^{-\frac{\alpha_A}{\lambda_A}}, x - \frac{\beta_A}{\lambda_A} \ln \left( \frac{y}{z_A} \right) \right) = (r, \theta),$$

$$(6) \quad \varphi_B(r, \theta) = \left( \theta - \frac{\beta_B}{\alpha_B} \ln \left( \frac{r}{r_B} \right), z_B \left( \frac{r}{r_B} \right)^{-\frac{\lambda_B}{\alpha_B}} \right) = (x, y).$$

Without loss of generality, we take  $\phi_{AB}$  to be the identity map. With the simplifying assumptions  $r_A = r_B$  and  $z_A = z_B = z_1$  we get the coordinates  $(x, y)$  of  $\Phi$ :

$$(7) \quad \Phi(x, y) = (\Phi_1(x, y), \Phi_2(x, y)) = (x + c_1 \ln y + c_2, c_4 y^{c_3})$$

where

$$c_1 = \frac{\alpha_A \beta_B - \beta_A \alpha_B}{\lambda_A \alpha_B} \quad c_2 = -c_1 \ln z_1 \quad c_3 = \frac{\alpha_A \lambda_B}{\lambda_A \alpha_B} \quad c_4 = z_1^{(1-c_3)}.$$

By the hypotheses (H1, H2),  $c_1 < 0$  and by (H1, H3) we have  $c_3 = 1$ ,  $c_4 = 1$ . Hence,  $\Phi(x, y) = (x + c_1 \ln y + c_2, y)$ . Thus,  $\Phi$  maps a vertical segment  $(x_1, u)$ ,  $0 < u < y_0$  on the wall  $\mathcal{W}_A$  into a helix that winds around  $\mathcal{W}_B$  and accumulates on the circle  $\mathcal{W}_{B_0}$  as  $u \rightarrow 0$  — see Figure 3. The image of another vertical segment,  $\Phi(x_2, u)$ ,  $0 < u < y_0$  may be obtained from that of the first segment by displacing the helix around the cylinder by an angle  $(x_2 - x_1)$ .

A rectangle  $[x_1, x_2] \times [Ky_2, y_2]$  in  $\mathcal{W}_A^+$  with  $y_2 > 0$ ,  $0 < K < 1$  is mapped into the region delimited by two helices. Its image makes a complete turn around the cylinder when  $K = e^{2\pi/c_1} = e^{-\pi\lambda_A/\beta_A}$ . Thus the image of a rectangle  $R_p^+ = [-w, w] \times [0, y_0]$  meets any neighbourhood of  $q$ .  $\square$

Note that if we had taken the rotation in  $N_B$  with the opposite orientation, then the two rotations in  $\varphi_A$  and  $\varphi_B$  would cancel out and we would obtain the identity map as the first order approximation of  $\Phi$ .

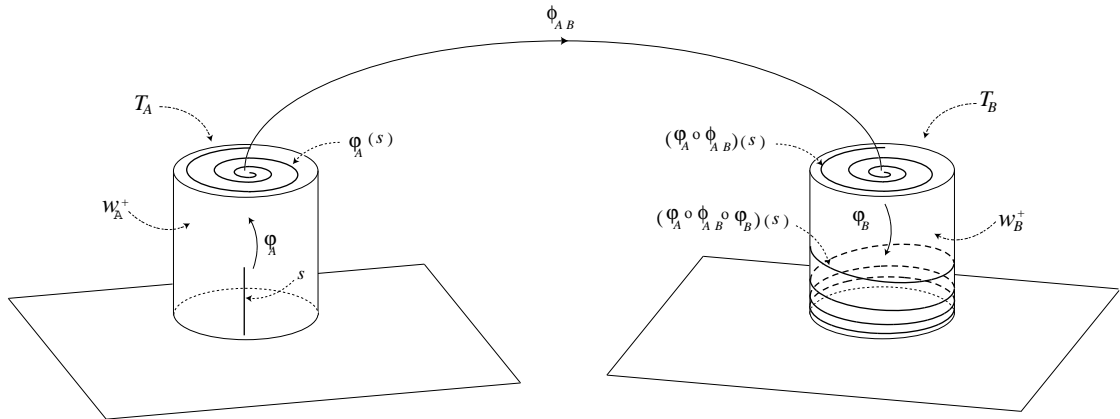


FIGURE 3. Geometry of  $\Phi = \varphi_B \circ \phi_{AB} \circ \varphi_A$ .

Our choice of orientation reflects what is observed numerically in Field's example.

We adapt the definition of horizontal and vertical strips in Guckenheimer and Holmes [16], chapter 5 to serve our purposes:

In a rectangle  $R = [-w, w] \times [-h, h]$ , a *vertical curve*  $x = v(y)$  is a curve for which

$$-w \leq v(y) \leq w \quad |v(y_1) - v(y_2)| \leq \mu |y_1 - y_2| \quad \text{in} \quad -h \leq y_1 \leq y_2 \leq h,$$

for some  $0 < \mu < 1$ . Similarly, a *horizontal curve*  $y = h(x)$  is one for which

$$-h \leq h(x) \leq h \quad |h(x_1) - h(x_2)| \leq \mu |x_1 - x_2| \quad \text{in} \quad -w \leq x_1 \leq x_2 \leq w,$$

for some  $0 < \mu < 1$ .

Given two nonintersecting vertical curves  $v_1(y) < v_2(y)$ ,  $y \in [-h, h]$  and two nonintersecting horizontal curves  $h_1(x) < h_2(x)$ ,  $x \in [-w, w]$ , we define *vertical* and *horizontal strips*, respectively, as

$$V = \{(x, y) : x \in [v_1(y), v_2(y)], y \in [-h, h]\}$$

$$H = \{(x, y) : x \in [-w, w], y \in [h_1(x), h_2(x)]\}.$$

Note that, in some instances, we shall use the generic word *strip* for a subrectangle.

**Proposition 3.** *Let  $X$  be a vector field satisfying (H0–H6). Let  $p_1, p_2 \in \mathcal{W}_{A_0}$  be points in the connections  $[B \rightarrow A]$  (in the same or in different connections). Then, for sufficiently small rectangles  $R_{p_j} \subset \mathcal{W}_A$  centered at  $p_j$  of width  $w_j$ ,  $j = 1, 2$ , there are two sequences  $(z_i)$  and  $(y_i)$  with  $\lim_{i \rightarrow \infty} z_i = 0$  and  $0 < y_{i+1} < z_{i+1} < y_i < z_i$  such that the transition map  $\Psi = \phi_{BA} \circ \varphi_B \circ \phi_{AB} \circ \varphi_A$  is well defined in the strips  $[-w_1, w_1] \times [y_i, z_i] \subset R_{p_1}$  and  $\Psi$  maps each horizontal strip in  $R_{p_1}$  into*

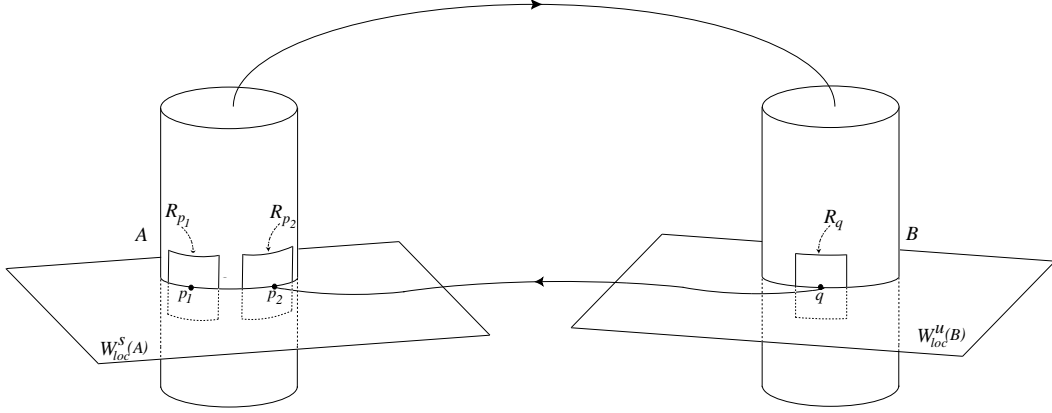


FIGURE 4. Geometrical setting of Proposition 3.

a vertical strip across  $R_{p_2}$ . Moreover, in suitable coordinates in  $R_{p_1}$  and  $R_{p_2}$  we may take in each strip:

$$\Psi(x, y) = (-y, x + c_1 \ln(y) + c_2) = (\tilde{x}, \tilde{y}) \pmod{2\pi}$$

where the constants  $c_1 < 0$  and  $c_2$  are the same as in Proposition 2.

**Proof:** Let  $q \in \mathcal{W}_{B_0}$  be such that the trajectory through  $q$  arrives at  $p_2$  — see Figure 4. We choose local coordinates  $(x, y)$  in  $\mathcal{W}_A$  and  $\mathcal{W}_B$  with  $p_1$  and  $q$  at the origin, so  $R_{p_1} = [-w_1, w_1] \times [-h_1, h_1]$  for some  $h_1 > 0$ .

Let  $h_2$  and  $w_2$  be the height and width, respectively, of  $R_{p_2}$  and consider a rectangle  $R_q \in \mathcal{W}_B$  centered at  $q$ , of height  $h_3 = w_2$  and width  $w_3 = h_2$ .

First we obtain strips in  $R_{p_1}^+$  that are mapped by  $\Phi$  across  $R_q$ . Using the expression (7) for  $\Phi$ , let  $z_i$  be the largest value of  $u$  such that  $\Phi_1(w_1, u) = -w_3 \pmod{2\pi}$  with  $0 < u < y_{i-1}$  (for  $i = 1$  take  $0 < u < \min\{h_1, h_3\}$ ). This value always exists, since  $u \mapsto \Phi(w_1, u)$  makes a complete turn around the cylinder when  $Ky_{i-1} \leq u \leq y_{i-1}$  as remarked at the end of the proof of Proposition 2. Now we take  $y_i$  as the largest value of  $u$  such that  $\Phi_1(-w_1, u) = w_3 \pmod{2\pi}$  with  $0 < u < z_i$ . Thus  $\Phi$  maps the horizontal strip  $[-w_1, w_1] \times [y_i, z_i]$  in  $R_{p_1}$  into the strip  $[-w_3 - 2w_1, w_3 + 2w_1] \times [y_i, z_i]$  in  $\mathcal{W}_B$ . This image contains the horizontal strip  $[-w_3, w_3] \times [f_1(x), f_2(x)]$  in  $R_q$ , where  $f_1(x) = \exp(x + w_1 - c_2)/c_1$  and  $f_2(x) = \exp(x - w_1 - c_2)/c_1$ .

We may assume, by shrinking the rectangles if necessary, that  $R_q$  is contained in a flow-box around the trajectory connecting  $q$  to  $p_2$ . The map  $\phi_{BA}$  is well defined in  $R_q$ . It follows that  $\Psi$  is well defined in the strips  $[-w_1, w_1] \times [y_i, z_i] \subset R_{p_1}$ .

Take coordinates  $(\tilde{x}, \tilde{y})$  in  $\mathcal{W}_A$  near  $p_2$  with  $p_2$  at the origin. As a simplification, we assume  $\phi_{BA}$  is a rotation of  $\pi/2$  and take  $q$  at the

origin of the coordinates in  $\mathcal{W}_B$ , to obtain using (7):

$$(8) \quad \Psi(x, y) = \left( -y, x + c_1 \ln \left( \frac{y}{z_1} \right) \right) = (\tilde{x}, \tilde{y}) \pmod{2\pi}$$

where  $c_1 \neq 0$  as before. The expression for  $\Psi$  is well defined only when  $\Phi(x, y)$  is near  $q$  and its coordinates are both defined modulo  $2\pi$ . Since  $R_{p_2}$  is the image by  $\phi_{BA}$  of  $R_q$  and  $h_2 = w_3$ , a strip  $[-w_1, w_1] \times [y_i, z_i] \subset R_{p_1}$  is mapped by  $\Psi$  across  $R_{p_2}$ .  $\square$

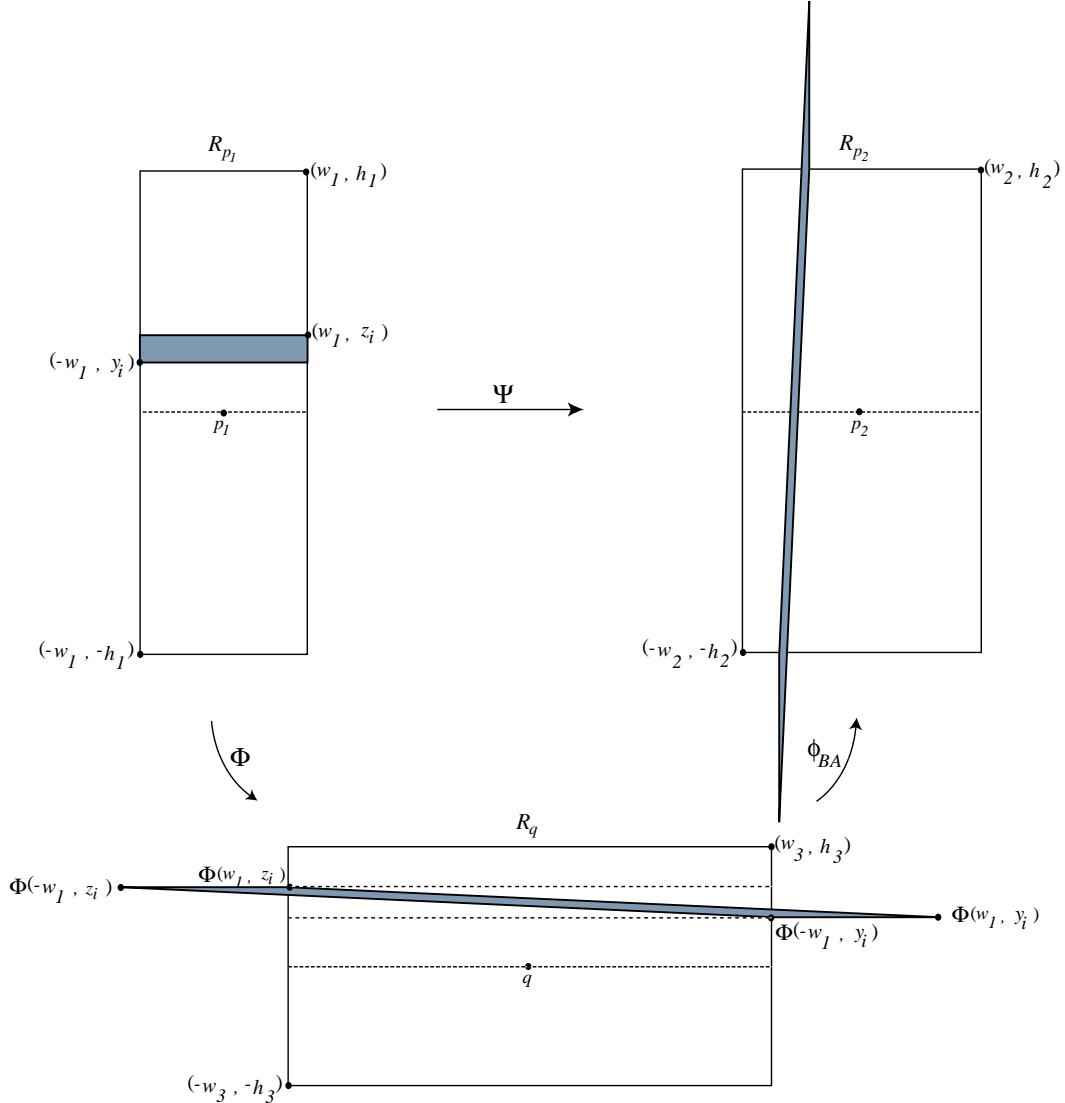


FIGURE 5. Geometry of the return map in Proposition 3

**6.1. Switching at nodes.** We are now able to describe the dynamics in a neighbourhood of a network such as the quotient network of

subsection 5.1. We start with switching at the nodes. The result is implicit in Propositions 2 and 3.

**Theorem 4.** *There is switching at the two nodes of a network of a vector field satisfying (H0–H6).*

**Proof:** First we show that switching at  $A$  follows directly from (H0), (H1) and (H6). Let  $q$  be a point in one of the connections  $[B \rightarrow A]$ . Any sufficiently small neighbourhood of  $q$  is contained in a flow-box around the connection and so it is mapped by the flow into  $\mathcal{W}_B$  either in small positive or in small negative time, so we may suppose  $q \in \mathcal{W}_B$ . Any neighbourhood of  $q$  contains a connected arc  $N_0$  such that  $q \in N_0 \subset \mathcal{W}_{B_0}$ . Transversality of the intersection of the 2-manifolds implies that there are points in  $N_0$  that are mapped by the flow into  $\mathcal{W}_A^+$  (and then follow the connections  $[A \rightarrow B]$  through  $\mathcal{T}_A, \mathcal{T}_B$ ) and also points that go to  $\mathcal{W}_A^-$ , and then follow the flow through  $\mathcal{B}_A, \mathcal{B}_B$ . Thus, there is switching at  $A$ .

Next, we use (H0), (H1), (H4) and (H5) to obtain switching at  $B$ . Points in a neighbourhood of the connection from  $\mathcal{T}_A$  to  $\mathcal{T}_B$  are mapped by the flow into a neighbourhood of the origin of  $\mathcal{T}_B$ . Consider any ray  $(r, \theta_0)$  in  $\mathcal{T}_B$ ,  $\theta_0$  fixed,  $0 < r < r_0$ . Using (6) it is easy to see that this ray is mapped by  $\varphi_B$  into a helix, similar to those in Figure 3, that accumulates on all of  $\mathcal{W}_{B_0}$  as  $r \rightarrow 0$ . For instance, the points  $(r, 0) \in \mathcal{T}_B$  are mapped by  $\varphi_B$  into

$$\varphi_B(r, 0) = \left( \frac{\beta_B}{\alpha_B} \ln r + c, z_B \left( \frac{r}{r_B} \right)^{-\frac{\lambda_B}{\alpha_B}} \right) = (x, y)$$

where the coordinate  $x$  in the cylinder wall  $\mathcal{W}_B$  is taken modulo  $2\pi$ . In particular, for each one of the  $m$  connections  $[B \rightarrow A]$  there are points  $(r, 0) \in \mathcal{T}_B$  that follow the given connection.

For trajectories near  $[A \rightarrow B]$  that go from  $\mathcal{B}_A$  to  $\mathcal{B}_B$  the same result holds, with the same proof.  $\square$

Note that to establish switching at  $A$ , we have exhibited trajectories that lie in  $W^u(B)$  and therefore these trajectories do not follow the network in negative time. This exemplifies the fact that switching at all nodes does not guarantee switching on the network. We are not using all the information available, as will be clear in subsection 6.4 below.

**6.2. Horseshoe geometry.** Now we address the special case of points in a neighbourhood of a connection  $[B \rightarrow A]$  that return to a neighbourhood of the same connection. This corresponds to the case  $p_1 = p_2$  in Proposition 3.

The next result shows that the return map  $\Psi$  has the geometrical behaviour of a horseshoe. We use the same coordinates as in the proofs

of Propositions 2 and 3. In these coordinates we have obtained an expression for  $\Psi$  and the expression is the same, independently of the connection considered.

**Corollary 5.** *Let  $X$  be a vector field satisfying (H0–H6). Let  $p \in \mathcal{W}_{A_0}$  be a point in one of the connections  $[B \rightarrow A]$  and  $R_p$  a rectangle centered at  $p$ . Then, there is a rectangle  $R = [-\nu, \nu] \times [y, z] \subset R_p$  with  $\nu > 0$  and  $z > y > 0$  such that there are two horizontal strips  $H_i \subset R$ ,  $i = 1, 2$  such that  $\Psi$  is well defined in each strip  $H_i$  and  $\Psi(H_i) \cap R$  is a vertical strip across  $R$ .*

**Proof:** Reducing  $R_p$  if necessary, suppose it is sufficiently small so we may apply Proposition 3 with  $p = p_1 = p_2$  and  $R_p = R_{p_1} = R_{p_2}$ ,  $w = w_1 = w_2$  to obtain two sequences  $(z_j)$  and  $(y_j)$ . The result follows from Proposition 3.  $\square$

We point out that the horseshoe in Corollary 5 lies between heights  $y$  and  $z$ . Applying the Corollary to another rectangle  $R_p$  of height less than  $y$ , we obtain another horseshoe, and therefore there is an infinite number of horseshoes accumulating on the connection.

**6.3. Hyperbolicity.** Let  $\Psi$  be the transition map from a strip contained in a rectangle centered at a connection point into another rectangle centered at another connection point. We have seen in the proof of Proposition 3 that in suitable coordinates these maps all have the same expression.

In this section we show that  $\Psi$  is hyperbolic in the sense defined below. When  $\Psi$  is a return map on a rectangle centered at a connection point, i.e. when the two connection points are the same, this guarantees that the invariant sets of the Poincaré map  $\Psi$  are Cantor sets, where the dynamics is conjugated to a shift on infinite sequences of two symbols. Hyperbolicity of the transition map  $\Psi$  between different rectangles is important to establish persistence of the dynamics and switching on the network, and will be used in 6.4 below.

We say that  $\Psi$  is *hyperbolic* at a point  $(x, y)$  if both  $\Psi$  and  $\Psi^{-1}$  are well defined at  $(x, y)$  and if there is  $\delta$ ,  $0 < \delta < 1$  such that, in suitable coordinates:

- The sector-bundle  $S^u = \{(v_1, v_2) : |v_1| < \delta|v_2|\}$  is invariant by  $D\Psi|_{(x,y)}$ , that is,  $D\Psi|_{(x,y)}(S^u) \subset S^u$ .
- The sector-bundle  $S^s = \{(v_1, v_2) : |v_2| < \delta|v_1|\}$  is invariant by  $D\Psi^{-1}|_{(x,y)}$ , that is,  $D\Psi^{-1}|_{(x,y)}(S^s) \subset S^s$ .
- For  $(v_1, v_2) \in S^u$ , if  $D\Psi|_{(x,y)}(v_1, v_2) = (w_1, w_2)$  then  $|w_2| \geq \frac{1}{\delta}|v_2|$ .
- For  $(v_1, v_2) \in S^s$ , if  $D\Psi^{-1}|_{(x,y)}(v_1, v_2) = (u_1, u_2)$  then  $|u_1| \geq \frac{1}{\delta}|v_1|$ .

**Theorem 6.** *Assume hypotheses (H0–H6) hold. Let  $p_1, p_2 \in \mathcal{W}_A$  be connection points and let  $R_{p_i}$  be open rectangles of height  $h \leq -c_1/2$*

centered at  $p_i$ . Then the Poincaré map  $\Psi$  from  $R_{p_1}$  to  $R_{p_2}$  is hyperbolic at all points in  $R_{p_1}$  where it is well defined.

**Proof:** Let  $p = p_1$ . It is sufficient to verify hyperbolicity at points  $(x, y)$  in the strips of Proposition 3 but we will consider any point  $(x, y)$  in  $R_p$ .

Using (8) at a point  $(x, y) \in R_p$ , we get

$$D\Psi|_{(x,y)} = \begin{bmatrix} 0 & -1 \\ 1 & \frac{c_1}{y} \end{bmatrix}, \quad D\Psi^{-1}|_{(x,y)} = \begin{bmatrix} \frac{c_1}{y} & 1 \\ -1 & 0 \end{bmatrix}.$$

Note that the symmetry  $(w_1, w_2) \mapsto (w_2, w_1)$  transforms  $D\Psi$  into  $D\Psi^{-1}$ . Therefore all results proved for  $D\Psi$  hold for  $D\Psi^{-1}$  with coordinates interchanged.

We obtain explicit expressions for the eigenvalues and eigenvectors of  $D\Psi$  in Lemma 7 below. The invariance of sector bundles is shown in Lemma 8 and the expansion property in Lemma 9.  $\square$

**Lemma 7.** *Under the conditions of Theorem 6, the derivative  $D\Psi|_{(x,y)}$  at a point  $(x, y) \in R_p$ , such that  $0 < y < -c_1/2$ , has real eigenvalues  $\mu_u$  and  $\mu_s$  satisfying  $\mu_u < -1 < \mu_s < 0$  with eigenvectors  $v_u = (-\mu_s, 1)$  corresponding to  $\mu_u$ , and  $v_s = (1, -\mu_s)$  corresponding to  $\mu_s$ .*

**Proof:** The eigenvalues of  $D\Psi|_{(x,y)}$  can be computed directly:

$$\mu_u = \frac{c_1}{2y} - \sqrt{\left(\frac{c_1}{2y}\right)^2 - 1} \quad \text{and} \quad \mu_s = \frac{c_1}{2y} + \sqrt{\left(\frac{c_1}{2y}\right)^2 - 1}.$$

Since  $0 < y < -c_1/2$ , the two eigenvalues are real. That  $\mu_s < 0$  follows from

$$\sqrt{\left(\frac{c_1}{2y}\right)^2 - 1} < \left|\frac{c_1}{2y}\right| = \frac{-c_1}{2y}.$$

Since  $c_1/2y < -1$  and  $1 + \sqrt{1 - 4\frac{y^2}{c_1^2}} > 1$  it follows that  $\mu_u < -1$ . On the other hand, it is easy to check the  $\mu_s > -1$  is equivalent to  $c_1/2y < -1$ . An eigenvector of  $D\Psi|_{(x,y)}$  corresponding to the eigenvalue  $\mu$  has the form  $(-1/\mu, 1)$ . The expressions for  $v_u$  and  $v_s$  follow since  $\mu_s\mu_u = \det D\Psi|_{(x,y)} = 1$ .  $\square$

From the expressions for the eigenvalues it follows that

$$\lim_{y \rightarrow 0} \mu_u = -\infty \quad \text{and} \quad \lim_{y \rightarrow 0} \mu_s = 0$$

and that, moreover, the eigenspaces define limit directions:

$$\lim_{y \rightarrow 0} \frac{v_u}{|v_u|} = (0, 1), \quad \text{and} \quad \lim_{y \rightarrow 0} \frac{v_s}{|v_s|} = (1, 0).$$

Choose the invariant sectors  $S^u$ , near the vertical direction, and  $S^s$ , near the horizontal direction, and define them as above.

**Lemma 8.** *With the hypotheses of Theorem 6, with  $-\mu_s < \delta < 1 < -\mu_u$  and  $(x, y) \in R_p^+$ , then  $D\Psi_{|(x,y)}(S^u) \subset S^u$  and  $D\Psi_{|(x,y)}^{-1}(S^s) \subset S^s$ .*

**Proof:** We show the invariance of  $S^u$ ; the result for  $S^s$  follows by symmetry. It is sufficient to show that  $(\delta, 1)$  and  $(-\delta, 1)$  are mapped by  $D\Psi_{|(x,y)}$  inside the same component of  $S^u$  — the invariance follows by linearity.

Since  $(x, y) \in R_p^+$  it follows that  $d = c_1/2y < -1$ . With this notation the eigenvalues of  $D\Psi_{|(x,y)}$  are  $\mu_s = d + \sqrt{d^2 - 1}$  and  $\mu_u = d - \sqrt{d^2 - 1}$ . We have  $-\mu_s + 2d = \mu_u$  and  $-\mu_u + 2d = \mu_s$ .

Consider first the image of  $(\delta, 1)$ , given by  $(v_1, v_2) = (-1, \delta + 2d)$ . Then  $v_2 = \delta + 2d < -\mu_u + 2d = \mu_s < 0$  and therefore  $-\mu_s < |v_2| = -v_2$ . Since  $0 < -\mu_s < \delta$ , then  $|v_1| = 1 < \mu_s^2 < \delta|v_2|$  showing that  $(v_1, v_2)$  lies in  $S^u$ .

Analogously, we show that the image of  $(-\delta, 1)$ , given by  $(w_1, w_2) = (-1, -\delta + 2d)$ , lies in  $S^u$ .

Finally, since both  $v_2$  and  $w_2$  are negative, they lie in the same component of  $S^u$ , proving the result.  $\square$

**Lemma 9.** *Denote  $D\Psi_{|(x,y)}(v_1, v_2)$  by  $(\omega_1, \omega_2)$  and  $D\Psi_{|(x,y)}^{-1}(u_1, u_2)$  by  $(\nu_1, \nu_2)$ . Under the conditions of Theorem 6, if  $-\mu_s < \delta < 1 < -\mu_u$ , for  $(x, y) \in R_p^+$ ,  $(v_1, v_2) \in S^u$  and  $(u_1, u_2) \in S^s$  then  $|w_2| \geq \frac{1}{\delta}|v_2|$  and  $|\nu_1| \geq \frac{1}{\delta}|u_1|$ .*

**Proof:** We show the result for  $S^u$  and  $D\Psi$ , the other case follows from symmetry. We have  $D\Psi_{|(x,y)}(v_1, v_2) = (\omega_1, \omega_2) = (-v_2, v_1 + 2dv_2)$  with  $d = c_1/2y$ . The expansion condition is

$$|v_1| < \delta|v_2| \quad \implies \quad \delta|v_1 + 2dv_2| = \delta|\omega_2| \geq |v_2|.$$

For this it is sufficient to show that  $(\delta, 1)$  and  $(-\delta, 1)$  lie in the same component of the sector defined by  $\delta|v_1 + 2dv_2| \geq |v_2|$ .

Since  $\delta < -\mu_u = -d + \sqrt{d^2 - 1} < -2d$ , then  $\delta + 2d < 0$ . For  $(v_1, v_2) = (\delta, 1)$  we obtain

$$\delta|v_1 + 2dv_2| - |v_2| = \delta|\delta + 2d| - 1 = -(\delta^2 + 2d\delta + 1).$$

The roots of  $\delta^2 + 2d\delta + 1 = 0$  are  $-\mu_s$  and  $-\mu_u$  and so  $-(\delta^2 + 2d\delta + 1) > 0$  if  $-\mu_s < \delta < -\mu_u$ . It follows that  $(\delta, 1)$  lies in the  $v_2 > 0$  component of the sector.

Analogously, we prove that  $(-\delta, 1)$  lies in the  $v_2 > 0$  component of the sector.  $\square$

Corollary 5 and the case  $p_1 = p_2 = p$  of Theorem 6 guarantee the existence of horseshoe dynamics near the heteroclinic cycles in the quotient network. Near each cycle there is a suspended horseshoe that meets  $\mathcal{W}_A$  in a Cantor set. See Guckenheimer and Holmes [16], chapter 5 and Wiggins [27], chapter 2.

**Remark.** By (H6) there is a flow-invariant neighbourhood of the connection through  $p$  that meets  $\mathcal{W}_A$  in  $R_p$ . Using (H5), and by the stronger version of switching at  $A$  in the proof of Theorem 10 below, it follows that the suspended horseshoe is captured by the union of  $N_A$ ,  $N_B$  and the two flow-invariant neighbourhoods of the connections. file SwitchNet.tex

**6.4. Switching on the network.** The main result in this paper can now be proved: switching on a network like the quotient network of subsection 5.1. The proof follows the construction of Proposition 3 as a more complicated version of the proof of Corollary 5.

**Theorem 10.** *There is switching on any network of a vector field satisfying (H0–H6).*

**Proof:** Given a neighbourhood  $N_\Sigma$  of the network  $\Sigma$ , we may take the neighbourhoods  $N_A$ ,  $N_B$  of  $A$  and  $B$  as before, restricting them to intersections with  $N_\Sigma$  if necessary.

Let  $p_1, \dots, p_m$  be representative points in the connections  $[B \rightarrow A]$ , and let  $\varrho_+$ ,  $\varrho_-$  be points in the two connections  $[A \rightarrow B]$ . Using (H5) and (H6) we may take the  $p_i$  in  $\mathcal{W}_{A_0}$ ,  $\varrho_+$  in  $\mathcal{T}_A$  and  $\varrho_-$  in  $\mathcal{B}_A$  i.e.,  $\{p_1, \dots, p_m\} = \mathcal{W}_{A_0} \cap W_{loc}^u(B)$ ,  $\{\varrho_+\} = W_{loc}^u(A) \cap \mathcal{T}_A$  and  $\{\varrho_-\} = W_{loc}^u(A) \cap \mathcal{B}_A$ . In the coordinates we are using,  $\varrho_+$  is the origin of  $\mathcal{T}_A$ .

A path in  $\Sigma$  visits the nodes  $A$  and  $B$  alternately since there are no connections from a node to itself. Thus, paths in  $\Sigma$  may be represented by sequences  $(a_n)_{n \in \mathbf{Z}}$  where  $a_{2n} \in \{p_1, \dots, p_m\}$  and  $a_{2n+1} \in \{\varrho_+, \varrho_-\}$ .

The following stronger version of switching at the node  $A$  holds. Given  $h > 0$ , with  $h < z_A$ , consider the cylinder of height  $h$  in  $\mathcal{W}_A^+$ ; in coordinates  $(x, y)$  on  $\mathcal{W}_A$  this is  $\{(x, y) : 0 \leq y \leq h\}$ . Using the expression for  $\varphi_A$  in the proof of Proposition 2, it is easy to see that this cylinder is mapped inside a disk of radius  $r(h)$  in  $\mathcal{T}_A$  such that  $\lim_{h \rightarrow 0} r(h) = 0$  (actually,  $r(h)$  is an increasing function of  $h$ , with  $r(0) = 0$ ). Similarly, a cylinder of height  $h$  in  $\mathcal{W}_A^-$  is mapped inside a small disk in  $\mathcal{B}_A$ .

Let  $R_{p_j}$  be the rectangle centered at  $p_j$  of height  $h$  and width  $w$ . Points in  $R_{p_j}^+$  follow paths corresponding to the partial sequence  $a_0, a_1 = p_j, \varrho_+$  and those on  $R_{p_j}^-$  follow  $a_0, a_1 = p_j, \varrho_-$ .

By Proposition 3, if  $h$  and  $w$  are small enough, then there is a strip  $S_{j1}^+ = [-w, w] \times [y_1, z_1] \in R_{p_j}^+$  where the transition  $\Psi$  to  $R_{p_1}$  is well defined and maps the strip across  $R_{p_1}$ . Then Proposition 3 may be applied to the rectangle centered at  $p_j$  of width  $w$  and height  $y_1$ , to

obtain a second strip  $S_{j_2}^+ = [-w, w] \times [y_2, z_2] \in R_{p_j}^+$  with  $z_2 < y_1$  that is mapped across  $R_{p_2}$ . Repeating the procedure, we obtain in each  $R_{p_j}^+$ ,  $m$  strips  $S_{j_i}^+$  where the return to  $\mathcal{W}_A$  going through  $\mathcal{T}_A$  is well defined and maps  $S_{j_i}^+$  across  $R_{p_i}$ . Another  $m$  strips  $S_{j_i}^-$  in  $R_{p_j}^-$  may be obtained, where the return to  $\mathcal{W}_A$  going through  $\mathcal{B}_A$  is well defined and maps  $S_{j_i}^-$  across  $R_{p_i}$ . As in the usual horseshoe construction, points in the strips  $S_{j_i}^+$  follow paths corresponding to the partial sequence  $a_0, a_1, a_2 = p_j, \varrho_+, p_i$  and those on  $S_{j_i}^-$  follow  $a_0, a_1, a_2 = p_j, \varrho_-, p_i$ .

If  $h < -c_1/2$  then, by Theorem 6, the Poincaré map  $\Psi$  is hyperbolic in all the strips. It follows that the set

$$\Lambda = \bigcap_{k \in \mathbf{Z}} \left( \bigcup_{\substack{j,i=1 \\ \varepsilon=\pm}}^m \Psi^k (S_{j_i}^\varepsilon) \right)$$

is a Cantor set of points where the return to  $\bigcup R_{p_j}$  is well defined in forward and backward time for arbitrarily large times. The dynamics of  $\Psi$  in the invariant set  $\Lambda$  is conjugated to a full shift on the  $2m$  symbols,  $(p_j, \varrho_l)$  that represent paths in  $\Sigma$ . Each point in  $\Lambda$  will correspond to the path on the network that it follows in forward and backward time. This establishes the switching.  $\square$

**6.5. Shadowing.** Some of the results of this paper can be rephrased in terms of shadowing. We discuss this briefly, see §5.1 of [16], Chapter 1, §3 and Chapter 2 §3 of [2] for details and definitions.

Two connections  $[M_{-1} \rightarrow N], [N \rightarrow M_{+1}]$  at the same node  $N$  of a network  $\Sigma$  can be seen as a pseudo-orbit of  $X$ , by removing the parts of the connections that lie near  $N$ . Switching at  $N$  means that these pseudo-orbits can be shadowed.

A path on  $\Sigma$  can also be seen as a pseudo-orbit of  $X$ , with infinitely many discontinuities. Switching on  $\Sigma$  means that these infinite pseudo-orbits can also be shadowed.

This shadowing does not respect the time parametrization: the shadowing trajectory will have to spend some time near the node and this will introduce a time delay for each node. It might be possible to control the delay when shadowing a finite pseudo-orbit, by introducing bounds on the distance to the node.

For the discrete dynamical system defined by the return map  $\Psi$ , consider representative points  $\{p_1, \dots, p_m\} = \mathcal{W}_{A_0} \cap W_{loc}^u(B)$  of the connections  $[B \rightarrow A]$  defined in the proof of Theorem 10. Switching on the network means that any sequence  $(a_n)_{n \in \mathbf{Z}}$  of points  $a_n \in \{p_1, \dots, p_m\}$  can be shadowed by an orbit of  $\Psi$ . Moreover, the shadowing orbit may

be chosen to visit  $\mathcal{W}_A^+$  and  $\mathcal{W}_A^-$  in any prescribed order, as this corresponds to the flow following the two connections in  $[A \rightarrow B]$  in any prescribed order.

## 7. LIFTED DYNAMICS

In this section we describe the consequences of the results obtained in the previous section to the dynamics of the original flow. We discuss how to lift the dynamics from the quotient to the original network of equilibria.

For clarity we list next the attributes of the original vector field  $X$  that are going to be used here. All these have already been discussed for the vector field (1) with parameters satisfying (3), and the network of equilibria  $\Sigma$  given by the first two rows of Table 2.

♠ The finite group  $\Gamma$  acts orthogonally on  $S^3$ , with a subgroup  $G$  acting freely on  $S^3$ .

$X$  is a  $\Gamma$ -equivariant vector field on  $S^3$  with a  $\Gamma$ -invariant network of equilibria  $\Sigma$ .

For any two nodes  $n_1, n_2$  in  $\Sigma$  there is at most one trajectory connecting  $n_1$  to  $n_2$  in  $\Sigma$ .

The only element of  $G$  that fixes a node in  $\Sigma$  is the identity.

Under these assumptions we may lift Theorem 4 to the original network:

**Corollary 11.** *Let  $X$  be a vector field on  $S^3$  with a network of equilibria  $\Sigma$  satisfying ♠ and suppose the quotient network  $\tilde{\Sigma} = \Sigma/G$  on  $S^3/G$  for the quotient vector field  $\tilde{X} = X/G$  satisfies (H0–H6). Then there is switching at each node of  $\Sigma$ .*

**Proof:** This follows from the same arguments used in the proof of Theorem 4, after lifting Propositions 2 and 3 to the original vector field. Instead of repeating the arguments we note that since the action of  $G$  is free, then for each node  $n$  in  $\Sigma$  the natural projection  $\pi : S^3 \rightarrow S^3/G$  is a diffeomorphism that maps a neighbourhood of  $n$  onto a neighbourhood of  $\pi(n)$ . Local behaviour of the flow, like switching at node  $n$ , is preserved by  $\pi$  and by its local inverse.  $\square$

Switching on the network is not a local property and thus its lifting requires more work. We start by lifting paths on the network.

**Lemma 12.** *Let  $X$  be a vector field on  $S^3$  with a network of equilibria  $\Sigma$  satisfying ♠ and let  $\tilde{\Sigma} = \Sigma/G$  be the quotient network on  $S^3/G$  for the quotient vector field  $\tilde{X} = X/G$ . Then any two paths on  $\Sigma$  that coincide in one node and that drop down to the same path on  $\tilde{\Sigma}$  are the same.*

**Proof:** Two paths  $(c_j)_{j \in \mathbf{Z}}$  and  $(d_j)_{j \in \mathbf{Z}}$  on  $\Sigma$  drop down to the same path if for all  $j$  we have  $\pi(c_j) = \pi(d_j)$ , i.e. for each  $j \in \mathbf{Z}$  there is

$\gamma_j \in G$  such that  $c_j = \gamma_j.d_j$ . If  $c_j = [n_{j-1} \rightarrow n_j]$  and  $d_j = [m_{j-1} \rightarrow m_j]$  then in particular,  $n_j = \gamma_j.m_j$ .

Suppose that  $n_k = m_k$  for some  $k \in \mathbf{Z}$ . Then  $n_k = \gamma_k.m_k = m_k$  and thus, by hypothesis,  $\gamma_k$  is the identity. Therefore  $[n_k \rightarrow n_{k+1}] = [m_k \rightarrow m_{k+1}]$  and in particular  $n_{k+1} = m_{k+1}$ .

The same argument shows that if  $n_k = m_k$  then  $[n_{k-1} \rightarrow n_k] = [m_{k-1} \rightarrow m_k]$  and the result follows by induction.  $\square$

Thus any path on  $\tilde{\Sigma}$  lifts to a finite number of paths on  $\Sigma$ . If  $(c_j)_{j \in \mathbf{Z}}$  and  $(d_j)_{j \in \mathbf{Z}}$  are two such paths, then either they coincide, or for each  $j \in \mathbf{Z}$  the connections  $c_j$  and  $d_j$  are disjoint. For instance, for the network of equilibria given by the first two rows of Table 2, consider the case of a periodic path corresponding to a simple cycle in the quotient network, given by one choice of connection in  $[A \rightarrow B]$  and another in  $[B \rightarrow A]$ . For example, we may choose the connections  $G.[a \rightarrow b]$  and  $G.[b \rightarrow sa]$ . This cycle lifts to two disjoint simple cycles in the original network of equilibria. With our choice of connections it either lifts to the cycle

$$a \rightarrow b \rightarrow sa \rightarrow sb \rightarrow s^2a \rightarrow s^2b \rightarrow s^3a \rightarrow s^3b \rightarrow s^4a \rightarrow s^4b \rightarrow s^5a = a$$

or to a similar cycle with a minus sign everywhere. Any other path in  $\Sigma$  that drops to the same cycle in  $\tilde{\Sigma}$  can be obtained from one of those two by a shift. Note that the cycle  $G.[a \rightarrow -b]$  and  $G.[-b \rightarrow sa]$  lifts to a single cycle of twice the length, visiting all the saddles in  $\Sigma$ .

**Theorem 13.** *Let  $X$  be a vector field on  $S^3$  with a network of equilibria  $\Sigma$  satisfying  $\spadesuit$  and suppose the quotient network  $\tilde{\Sigma} = \Sigma/G$  on  $S^3/G$  for the quotient vector field  $\tilde{X} = X/G$  satisfies (H0–H6). Then there is a suspended horseshoe in any neighbourhood of each cycle in  $\Sigma$ .*

**Proof:** When we iterate  $\Psi$  we are following along a simple cycle in the quotient network: by Corollary 5 and Theorem 6 the quotient flow is a suspended horseshoe. From Lemma 12 it follows that the simple cycle lifts to a finite number of disjoint simple cycles in  $\Sigma$ . By the remark at the end of section 6.3, the suspended horseshoe is contained in flow-invariant neighbourhoods of the connections. The suspended horseshoe lifts to a suspended horseshoe that follows the lifted cycle.  $\square$

**Theorem 14.** *Let  $X$  be a vector field on  $S^3$  with a network of equilibria  $\Sigma$  satisfying  $\spadesuit$  and suppose the quotient network  $\tilde{\Sigma} = \Sigma/G$  on  $S^3/G$  for the quotient vector field  $\tilde{X} = X/G$  satisfies (H0–H6). Then there is switching in  $\Sigma$ .*

**Proof:** Without loss of generality, consider a  $\Gamma$ -invariant neighbourhood  $N_\Sigma$  of  $\Sigma$ , and take a  $\Gamma$ -invariant set of neighbourhoods of the nodes in  $\Sigma$ . These drop down to neighbourhoods  $N_{\tilde{\Sigma}}, N_A, N_B$  of  $\tilde{\Sigma}$  and of  $A$  and  $B$  respectively. The results of section 6 hold in these neighbourhoods, reducing them if necessary. Again without loss of generality, consider a  $\Gamma$ -invariant set of representative points of the connections in  $\Sigma$  and a  $\Gamma$ -invariant set of their neighbourhoods, that drop down to representative points  $q_j, j = 1, \dots, 10$  of all the ten connections in  $\tilde{\Sigma}$  and neighbourhoods  $N_{q_j}$  of the  $q_j$ .

Start with a path  $([m_{j-1} \rightarrow m_j])_{j \in \mathbf{Z}}$  on  $\Sigma$  that drops down to a path  $([M_{j-1} \rightarrow M_j])_{j \in \mathbf{Z}}$  on  $\tilde{\Sigma}$ .

By Theorem 10 the quotient path can be shadowed, inside  $N_{\tilde{\Sigma}}$ , by a trajectory  $\tilde{x}(t)$  of the quotient vector field  $\tilde{X}$ . More precisely, if  $p_j$  is the representative point  $p_j \in \{q_1, \dots, q_{10}\}$  that lies on the connection  $[M_{j-1} \rightarrow M_j]$ , then there are sequences  $(t_j), (s_j), j \in \mathbf{Z}$  with  $t_{j-1} < s_j < t_j$ , such that  $\tilde{x}(s_j) \in U_{p_j}$  and  $\tilde{x}(t_j) \in U_{M_j}$ .

Let  $x_0$  be a point in the neighbourhood of  $m_0 \in S^3$  satisfying  $\pi(x_0) = \tilde{x}(t_0) \in U_{M_0}$ , and let  $x(t)$  be the trajectory of  $X$  satisfying  $x(t_0) = x_0$ , and thus,  $\pi(x(t)) = \tilde{x}(t)$ . Using hypotheses (H5) and (H6), Theorem 10 can be stated and proved with flow-invariant neighbourhoods of the connections. The proof is complete since, by arguments like those in the proof of Lemma 12,  $x(t)$  follows the path  $([m_{j-1} \rightarrow m_j])_{j \in \mathbf{Z}}$ .  $\square$

**Acknowledgements.** The authors are grateful to Mike Field for very useful discussions and suggestions. These took place both in Houston and in Porto and benefitted from financial support from Fundação Luso-Americana para o Desenvolvimento and Fundação para a Ciência e a Tecnologia. Part of this work was done while the first author was on leave from the Faculdade de Economia do Porto and receiving a Prodep grant.

## REFERENCES

- [1] M.A.D. Aguiar, 2002, *Vector fields with heteroclinic networks*, Phd thesis Departamento de Matemática Aplicada, Faculdade de Ciências da Universidade do Porto
- [2] D.V. Anosov (ed), 1995, *Dynamical Systems IX — Dynamical Systems with Hyperbolic Behaviour*, Encyclopædia of Mathematical Sciences, vol 66 Springer-Verlag
- [3] D. Armbruster, E. Stone and V. Kirk, 2003, *Noisy Heteroclinic Networks*, Chaos, Vol. **13**, pages 71–79
- [4] P. Ashwin and P. Chossat, 1998, Attractors for Robust Heteroclinic Cycles with Continua of Connections, *J. Nonlinear Sci.*, Vol. **8**, pages 103–129
- [5] P. Ashwin and M. Field, 1999 *Heteroclinic Networks in Coupled Cell Systems* Arch. Rational Mech. Anal., **148**, pages 107–143

- [6] W. Brannath, 1994, *Heteroclinic networks on the tetrahedron*, Nonlinearity, Vol. **7**, pages1367–1384
- [7] S.A. Campbell and P. Holmes, 1991, *Bifurcation from  $O(2)$  symmetric heteroclinic cycles with three interacting modes*, Nonlinearity, **4**, pages 697–726
- [8] T. Chawanya, 1997, *Coexistence of infinitely many attractors in a simple flow*, Physica D, Vol. **109**, pages201–241
- [9] P. Chossat, F. Guyard and R. Lauterbach, 1999, *Generalized Heteroclinic Cycles in Spherically Invariant Systems and their Perturbations*, J. Nonlin. Science, Vol. **9**, Nr. **5**, pages479–524
- [10] A.P.S. Dias, B. Dionne and I. Stewart, 2000 *Heteroclinic Cycles and Wreath Product Symmetries* Dynamics and Stability of Systems, vol **15**, No **4**, pages 353–385
- [11] M.J. Field, 1980 *Equivariant Dynamical Systems* Transactions of the Amer. Math. Soc., Vol.**259**, No.**1**, pages 185–205
- [12] M.J. Field, 1989, *Equivariant bifurcation theory and symmetry breaking*, *J. Dynamics and Diff. Equations*, **1**, pages 369–421
- [13] M.J. Field, R.W. Richardson, 1992, *Symmetry-Breaking and Branching Patterns in Equivariant Bifurcation Theory, II*, Arch. Rational Mech. Anal., **120**, pages 147–190
- [14] M. Field and J.W. Swift, 1992, *Stationary bifurcation to limit cycles and heteroclinic cycles*, Nonlinearity, **4**, pages 1001–1043
- [15] M.J. Field, 1996, *Lectures on Bifurcations, Dynamics and Symmetry*, Pitman Research Notes in Mathematics Series 356, Longman
- [16] J. Guckenheimer and P. Holmes,1983, *Nonlinear Oscillations, Dynamical Systems, and Bifurcations of Vector Fields*, Applied Mathematical Sciences, number 42, Springer-Verlag
- [17] J. Guckenheimer, B.A. Meloon, M.R. Myers, F.J. Wicklin, P.A. Worfolk, 1997, *DsTool: A Dynamical System Toolkit with an Interactive Graphical Interface - User's Manual*,Version Tk Draft, Center for Applied Mathematics, Cornell University
- [18] J. Guckenheimer and P. Worfolk, 1992, *Instant Chaos*, Nonlinearity, **5**, pages 1211–1222
- [19] O. Junge, 2000 *GAIIO - Reference Manual Version 1.2* Department of Mathematics and Computer Science University of Paderborn
- [20] V. Kirk and M. Silber, 1994, *A competition between heteroclinic cycles*, Nonlinearity, **7** pages 1605–1621
- [21] M. Krupa, 1997, *Robust Heteroclinic Cycles*, J. Nonlinear Sci., **7**, pages 129–176
- [22] R. Lauterbach and M. Roberts, 1992, *Heteroclinic Cycles in Dynamical Systems with Broken Spherical Symmetry*, Journal of Differential Equations, **100**, pages 22–48
- [23] I. Melbourne, P. Chossat and M. Golubitsky, 1989 *Heteroclinic cycles involving periodic solutions in mode interactions with  $O(2)$  symmetry* Proc. of the Royal Soc. of Edinburgh, **113A**, pages 315–345
- [24] Ernst Reissner, 1999, *On flows with Spatio-Temporal Symmetries near Heteroclinic Networks*, Shaker Verlag, Augsburg University Dissertation
- [25] V.S. Samovol, 1972, *Linearization of a system of differential equations in the neighborhood of a singular point*, *Soviet Math. Dokl.*, Vol. **13**, No. **5**, pages 1255–1259
- [26] M. Silber, H. Riecke and L. Kramer, 1992, *Symmetry-breaking Hopf bifurcation in anisotropic systems*, Physica D, Vol. **61**, pages260–278

- [27] S. Wiggins, 1988, *Global Bifurcations and Chaos - Analytical Methods*, Springer-Verlag
- [28] P.A. Worfolk, 1996 *An Equivariant, Inclination-Flip, Heteroclinic Bifurcation* *Nonlinearity*, **9**, pages 631–647